Multinuclear MQMAS NMR Study of NH_4/Na-Ferrierites

Priit Sarv*

Institute of Chemical Physics and Biophysics, Akadeemia 23, EE0026 Tallinn, Estonia

Blanka Wichterlová and Jiří Čejka

J. Heyrovsky Institute of Physical Chemistry, Academy of Sciences of the Czech Republic, Dolejškova 3, CZ-182 23 Prague 8, Czech Republic

Received: September 16, 1997; In Final Form: December 7, 1997

(MQ)MAS NMR is a powerful new method to study quadrupolar nuclei, enabling separation of the chemical shift interaction from the quadrupolar interaction. We showed that hydrated NH_4-ferrierites have two distinct aluminum sites with an average ratio of 4:5. These sites were assigned to T(2) + T(3) and T(5) + T(1) + T(4) sites, respectively. Upon increase of the aluminum content, the ratio 4:5 remained the same. At higher Si/Al ratios, aluminum tends to form aluminum-rich zones, leaving some unit cells without aluminum atoms. Na^+ exchange decreases the average T−O−T angles of the aluminum sites. It has been found that Na^+ ions are preferentially located in the "ferrierite cages", formed at the intersection of six-membered ring channels and eight-membered ring channels.

Introduction

A potential application of crystalline aluminosilicates with the ferrierite/ZSM-35 structure as catalysts for isomerization of linear butenes to isobutene,[1,2] and for NO*x* abatement by employing cobalt loaded ferrierites for selective catalytic reduction of NO by methane in an oxygen excess,[3] has currently drawn to them considerable attention. Besides the defined intracrystalline volume and channel architecture playing an important role in shape-selective catalytic processes (like skeletal isomerization of *n*-butenes[1]), aluminum distribution in high-silica frameworks of ferrierites seems to be of high importance, as it controls density and distribution of both the protonic and metal ion sites. Moreover, local Si/Al ordering in high-silica zeolites affects, besides the metal ion siting,[4] their redox properties and catalytic activity, as shown, for example, for Cu−ZSM-5.[5−7]

Ferrierites are medium-pore zeolites with a crossing 8-ring and 10-ring channel system.[8] The crystal structure of ferrierite was first solved by Vaughan[9] on a magnesium-containing mineral sample from Kamloops Lake, Canada, and has been confirmed by a number of other workers.[10,11] The unit cell (UC) was reported to contain four nonequivalent tetrahedral (T) sites. Recently, the structure of a siliceous ferrierite was refined, where the UC comprised 5 nonequivalent T sites.[12,13] The structure of siliceous ferrierite can serve as a starting point for the interpretation of the ^{29}Si MAS NMR spectra of the aluminosilicate forms of ferrierite, after making some assumptions about the distribution of Al in the framework.[12,14] If we could get direct evidence about the distribution of Al from the ^{27}Al MAS NMR data, we could be more convinced about our conclusions.

Metal ions at exchangeable sites, as they are adjacent to the framework Al atoms (AlO_4^-) bearing local negative charge, can be expected to induce local structural changes at this Al framework site. The changes, induced by the cations, can be studied by ^{29}Si MAS NMR, as done in the case of low Si/Al ratio zeolites A, X, and Y.[15] But since the structural changes are expected to be around the tetrahedral aluminum atom, ^{27}Al NMR should be the proper technique for the characterization.

The application of ^{27}Al MAS NMR is hampered because the information about the distribution of Al sites, contained in the spectrum, is obscured by the second-order broadening and the line shift of ^{27}Al resonances due to the quadrupolar effects. A new two-dimensional (2D) NMR technique, multiquantum MAS experiment of quadrupolar nuclei (MQMAS NMR),[16,17] has made it possible to separate the chemical shift interaction (CS) from quadrupolar interaction (QI), and the distribution of Al sites is given by the isotropic projection. Recently, this novel technique was applied to study aluminum distribution in ZSM-5 type zeolites,[18] and we are going to use it also for the ferrierite-type materials.

The same multiquantum technique (^{23}Na 3MQMAS NMR) can be used also to study Na^+ cation siting in the dehydrated zeolites.[19] By applying this technique to ferrierites with different Na^+ content, we hope to get information about the distribution and surrounding of the Na^+ ion.

Experimental Section

Materials. Na,K-ferrierite of Si/Al framework molar ratio of 8.4 was provided by TOSOH Co. Na-ferrierite (Si/Al 30) was synthesized using the following procedure. Pure silica (Cab-O-Sil M5) in NaOH solution was mixed with a solution of sodium sulfate and aluminum sulfate. In a final step pyridine as a template was added. The synthesis was carried out in a Teflon-lined stainless steel autoclave under autogenous pressure at 448 K for 70 h. The obtained solid phase was washed with deionized water, filtered and dried at 373 K. XRD analysis proved well-crystalline samples and SEM showed crystals of the dimension of about 10 × 10 × 3 μm. Both the zeolites were five times ion exchanged with 0.5 M NH_4NO_3 at room temperature to complete the exchange of all the cations for NH_4^+ ions. NH_4-ferrierite with Si/Al = 8.4 was again exchanged with a 0.1 M NaCl several times to obtain NH_4Na-ferrierites with

S1089-5647(97)03028-9 CCC: $15.00
Published on Web 01/30/1998

TABLE 1: Composition of the NH_4^+/Na^+-Ferrierites

sample	Si/Al[a] molar chemical analysis	Si/Al molar NMR	OH groups[b] mmol/g	Na^+ (%)[c]
NH_4-ferri/30	30	33	0.49	0
NH_4-ferri/8.4	8.4	7.9−8.4	1.75	0
NH_4Na-ferri/8.4-14	8.4	7.7−8.7	1.50	14
NH_4Na-ferri/8.4-20	8.4		1.40	20
NH_4Na-ferri/8.4-83	8.4	8.1−8.4	0.30	83
NH_4Na-ferri/8.4-100	8.4		0	100

[a] Chemical analysis by atomic absorption spectrometry after dissolution. [b] Bridging OH groups determined by FTIR spectra of OH groups at 3605 cm^{-1} and temperature-programmed desorption of ammonia after zeolites evacuation at 720 K for 3 h (details in ref 4). [c] Degree of NH_4^+ replaced by Na^+.

different content of Na^+ ions. The composition of ferrierites is given in Table 1. The ^{27}Al MAS NMR showed that in all the samples 100% of Al was in the framework. Identification of the samples is as follows: NH_4-ferri/8.4 means ammonium form of ferrierite with Si/Al = 8.4, NH_4,Na-ferri/8.4-14 denotes sample with Si/Al = 8.4 and 14% of NH_4^+ exchanged by Na^+ ions.

NMR. The MAS NMR spectra were measured on Bruker AMX500 spectrometer using homemade probeheads with 3.5 mm o.d. rotors and 4.0 mm o.d. rotors. The spinning speed was between 12 and 15 kHz. For ^{27}Al NMR experiments AMX500 was equipped with an additional 250 W power amplifier to ensure the radio frequency (rf) field strength of 120 kHz. $KAl(SO_4)_2 \cdot 12H_2O$ was used as an external reference for ^{27}Al (δ_{CS} = 0 ppm relative to $Al_2(NO_3)_3$ 1 M aqueous solution) and to measure the rf power. ^{29}Si MAS NMR spectra were recorded with a 45° flip angle and with a 30 s repetition delay. ^{29}Si chemical shifts were referenced relative to TMS with an external standard HMDSO (^{29}Si CS = 6.5 ppm relative to TMS). 2D ^{23}Na 3Q MAS NMR spectra were recorded in a 360 MHz (^{1}H NMR frequency) magnet, and an additional amplifier (Bruker CXP) was used to boost the rf strength up to 230 kHz. 1D ^{23}Na MAS NMR experiments were carried out in a 500 MHz (^{1}H NMR frequency) magnet with a 15° pulse and 0.5 s delay. ^{23}Na chemical shifts were referenced relative to aqueous solution of NaCl with an external reference NaCl (CS = 7.0 ppm). ^{23}Na NMR experiments were done on dehydrated samples, and ^{27}Al and ^{29}Si NMR experiments were done on hydrated samples (at least 48 h in 75% humidity). All 1D spectra were deconvoluted with a Bruker 1D WIN NMR package.

The 2D MQMAS experiments were performed with a two-pulse sequence. The first pulse has the length optimized to obtain the best efficiency for the multiquantum (±5Q for Al and ±3Q for Na) coherence creation. The second pulse is designed to transfer these two symmetrical coherences with the same efficiency into observable (−1)Q single-quantum coherence. With a proper phase-cycling, only the desired coherence transfer pathways (0)(±5 or ±3)(−1), were selected. Data were aquired with the States-TPPI method. Shearing transformation was done by employing a t_1-dependent first-order phase correction in the mixed (t_1, ν_2) domain, after constructing echo and antiecho signals.[20] After a subsequent F1 Fourier transform, the isotropic projection can be obtained from the ν_1^s (index s stands for "sheared") projection of the final 2D spectrum. In the ν_1^s projection the second-order broadening is eliminated now, but the second-order quadrupolar shifts are still present. In the zeolites the Al sites that occupy the same positions in the unit cell are not equal for the NMR experiment due to several reasons: random distribution of Al, positioning of the cations and adsorbates in the pores, just to mention some of them. So, zeolites are not perfectly crystalline, and therefore all Al sites have a small distribution of quadrupolar coupling parameters, instead of a distinct value. This causes some additional line broadening in the ν_1^s dimension of the order of 0.1−0.2 ppm, due to the distribution of the second-order quadrupolar shift. But the main broadening is still caused by the distribution of the chemical shift (Figure 3). In case of ill-crystallized or amorphous samples, the F1 resolution is enhanced with high MQ orders,[21] and therefore we used the highest possible MQ order in our 2D experiments (5Q for ^{27}Al and 3Q for ^{23}Na).

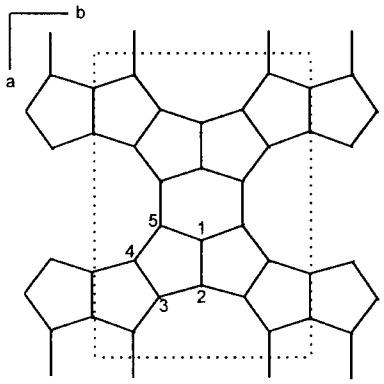

Figure 1. Ferrierite framework projected on *ab* plane. Tetrahedral sites are numbered as in ref 13.

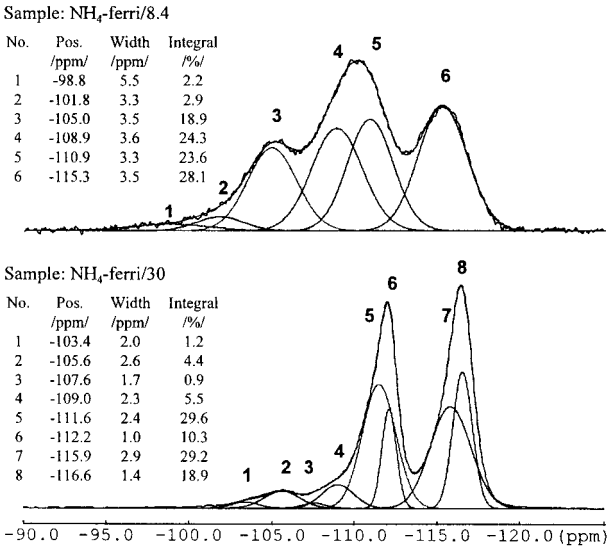

Figure 2. ^{29}Si MAS NMR spectra of samples NH_4-ferri/30 and NH_4-ferri/8.4 together with simulations.

Using the results in refs 16 and 17, we can deduce the effective Larmor frequency in the ν_1^s

$$\nu_0^s = \nu_0 \cdot |p - R|$$

where p is the coherence order and R the anisotropic ratio: for ^{23}Na $p = 3$ and $R = -7/9$; for ^{23}Al $p = 5$ and $R = -25/12$. Correct chemical shift reference in the ν_1^s dimension is obtained by setting the SF1 (Bruker notation) parameter equal to SF2·$|p - R|$ so that in the center point of the 2D spectrum, where the offset is zero, the chemical shifts (in ppm) of ν_1^s and ν_2 dimension are equal. Isotropic chemical shift and the quadrupolar shift can be derived from the equations

$$\delta_1^s = \delta_{CS} + C \cdot \delta_Q$$

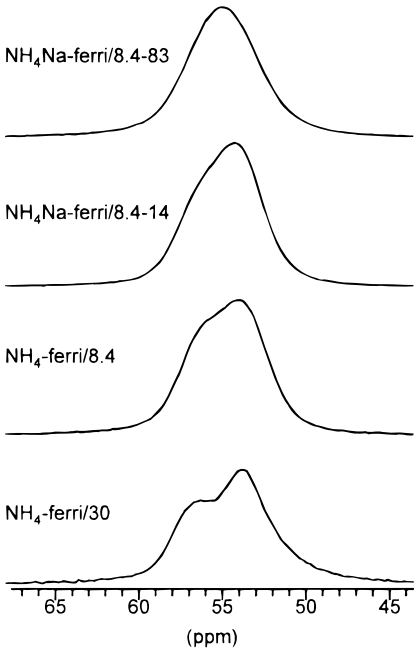

Figure 3. Center bands of the ^{27}Al MAS NMR spectra of samples NH_4-ferri/30, NH_4-ferri/8.4, NH_4Na-ferri/8.4-14, and NH_4Na-ferri/8.4-83.

$$\delta_2 = \delta_{CS} + \delta_Q$$

where δ_{CS}/ppm/ is the isotropic chemical shift, δ_Q/ppm/ is the quadrupolar shift, δ_1^s/ppm/ and δ_2/ppm/ are the coordinates of the centers of gravity of the 2D lines in the ν_1^s and ν_2 dimension, respectively; and $C = -10/17$ is a constant, which has the same value for the sheared 3Q ^{23}Na and 5Q ^{27}Al 2D spectra.

Results and Discussion

^{27}Al MAS NMR spectra of NH_4-ferrierites (Figure 3) give a maximum at 54 ppm and a well-resolved shoulder at lower shielding. Whether the shoulder reflects the CS distribution or the second-order quadrupolar line shape cannot be answered on the basis of the 1D spectum only. Moreover, the central band comprises not only the central transition ($-1/2$ to $1/2$) but also contributions from the satellite transitions ($\pm 3/2$ and $\pm 5/2$), which makes the analysis even more complicated. We need to separate the two interactions (CS and QI), and the 2D (MQ)-MAS NMR method is an appropriate way to do that. In Figure 4 there is the sheared ^{27}Al 2D 5Q (MQ)MAS NMR spectra of NH_4-ferri/30, NH_4-ferri/8.4, NH_4Na-ferri/8.4-14, and NH_4Na-ferri/8.4-83 together with projections. Quadrupolar line shapes are parallel to F2 or the anisotropic axis, and the chemical shift distribution is parallel to F1 or the isotropic axis. The F1 projection reflects the distribution of chemical shift. In our case this statement holds since all the sites have approximately the same value for the quadrupolar coupling (see Table 2), and therefore they all are detected to the same extent (see Figure 1 in ref 18). The distribution of quadrupolar coupling parameters induces some additional line broadening in the F1 dimension of the order of 0.1−0.2 ppm. One can see from Figures 4 and 5 that the F1 projection has a better resolution compared to 1D ^{27}Al MAS NMR spectra (Figure 3) and that on most spectra two Al sites can be resolved. The 2D coordinates of the centers of gravity of the lines, isotropic chemical shifts, and parameters describing the quadrupolar interaction of the sites are given in Table 2. From the isotropic chemical shift we calculated the average T−O−T bond angle and compared it with the T−O−T bond angle obtained from the ^{29}Si chemical shift (see Table 2). To calculate the Al T−O−T bond angle we used the equation $^{Al}\delta = -0.500 \cdot \bar{\alpha} + 132$[22] and for Si we used the relation $^{Si}\delta = -0.5793 \cdot \bar{\alpha} - 25.44$.[23] We note that these two empirical equations correlate the NMR data with the X-ray data, which in the case of aluminosilicate zeolites in general cannot distinguish between Al and Si tetrahedral sites. Therefore, the ambiguous notation T−O−T is used, instead of Al−O−Si or Si−O−Si. Also we do not consider the contribution from the T−O bond length change to the CS.[13]

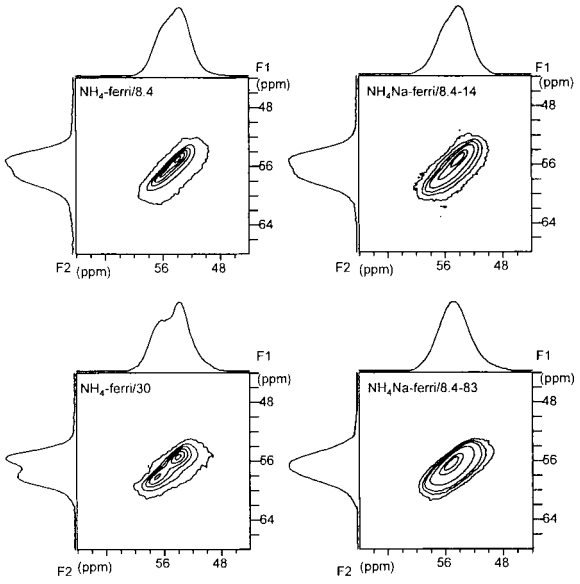

Figure 4. Sheared ^{27}Al 5Q (MQ)MAS NMR spectra of NH_4-ferri/30, NH_4-ferri/8.4, NH_4Na-ferri/8.4-14, and NH_4Na-ferri/8.4-83 together with the projections. F1 is the isotropic axis.

Interconnected silicon and aluminum tetrahedra (TO_4) form the ferrierite framework (Figure 1). While the bond angles inside the tetrahedra (O−T−O) are relatively stable, the angles between the tetrahedra (T−O−T) can take quite a broad range of values. There exist empirical formulas, which relate the T−O−T angle to the CS of aluminum and silicon and give us the opportunity to obtain information about the framework from two different sources.[22,23] In the following we compare the data from ^{29}Si and ^{27}Al NMR and discuss the conclusions about the structure. First we assign the ^{29}Si and ^{27}Al NMR spectra of low-aluminum ferrierite, NH_4-ferri/30, to specific T sites in the structure. Then we generalize the results to high-Al ferrierite, NH_4-ferri/8.4. Finally we study the effect of NH_4^+/Na^+ ion exchange on the Al T−O−T angles and the distribution of Na^+ ions in the framework.

^{29}Si MAS NMR of NH_4-Ferri/30. In the ^{29}Si MAS NMR spectrum of NH_4-ferri/30 (Figure 2) two main peaks, with the maxima at −112.2 and −116.6 ppm, can be clearly identified, which according to their chemical shift are assigned to Si(0Al) sites. A small shoulder at −109.0 (lines 3 and 4) and a small peak at −105.6 (lines 1 and 2) are assigned to Si(1Al) sites, giving the Si/Al ratio equal to 33, which is in reasonable agreement with the Si/Al = 30 from the chemical analysis. The resolution of five different Si sites, characteristic of the siliceous ferrierite,[12,13] is not achieved because of the disorder around each silicon atom created by substitution of aluminum into the framework. In the ^{29}Si MAS NMR spectrum of the calcined siliceous ferrierite, there are five peaks with intensity ratios 2:2:2:1:2 assigned to five nonequivalent tetrahedral sites (T sites) in the unit cell (UC).[12,13] If we group the sites with close chemical shifts, we get the sites of the type T(A) comprising

TABLE 2: Results of the 5Q (MQ)MAS NMR Characterization Together with Average T−O−T Angles Calculated from the ^{27}Al and ^{29}Si Chemical Shifts[a]

sample/site	F1/ppm/ ±0.1	F2/ppm/ ±0.1	$C\delta_Q$/ppm/ ±0.1	SOQE/ MHz/±0.1	$^{27Al}\delta_{CS}$/ ppm/±0.2	T−O−T^{Al}/deg ±0.4	$^{29Si}\delta_{CS}$/ppm/ ±0.2	T−O−T^{Si}/deg/ ±0.3
NH_4-ferri/30 /T(A)	58.1	56.9	0.5	1.5	57.6	148.7	−112.2$^{(nr.6)b}$	149.8
							−111.6$^{(nr.5)b}$	148.7
NH_4-ferri/30 /T(B)	55.4	54.0	0.5	1.6	54.9	154.3	−116.6$^{(nr.8)b}$	157.4
							−115.9$^{(nr.7)b}$	156.2
NH_4-ferri/8.4/T(A)	57.4	56.3	0.4	1.4	57.0	150.0	−110.9	147.5
NH_4-ferri/8.4/T(B)	54.8	53.7	0.4	1.4	54.4	155.2	−115.3	155.1
NH_4Na-ferri/8.4-14 /T(A)	57.4	56.1	0.5	1.5	56.9	150.2	−111.2	148.0
NH_4Na-ferri/8.4-14 /T(B)	54.8	53.7	0.4	1.4	54.4	155.2	−115.4	155.3
NH_4Na-ferri/8.4-83 /T[c]	56.4	55.1	0.5	1.5	55.9	152.1	−113.3	151.7

[a] F1, F2 are the coordinates of the peaks on the 2D spectrum; $C\delta_Q$ is the quadrupolar shift in the sheared dimension F1; SOQE = $C_q(1 + \eta^2/3)^{1/2}$ describes the quadrupolar interaction. [b] For sample NH_4-ferri/30 two components of the T(A) and T(B) peaks in ^{29}Si MAS NMR spectrum are given for comparison. [c] For sample NH_4Na-ferri/8.4−83 only average of the two sites is given, since T(A) and T(B) cannot be unambiguously resolved from the 5Q (MQ)MAS NMR spectrum.

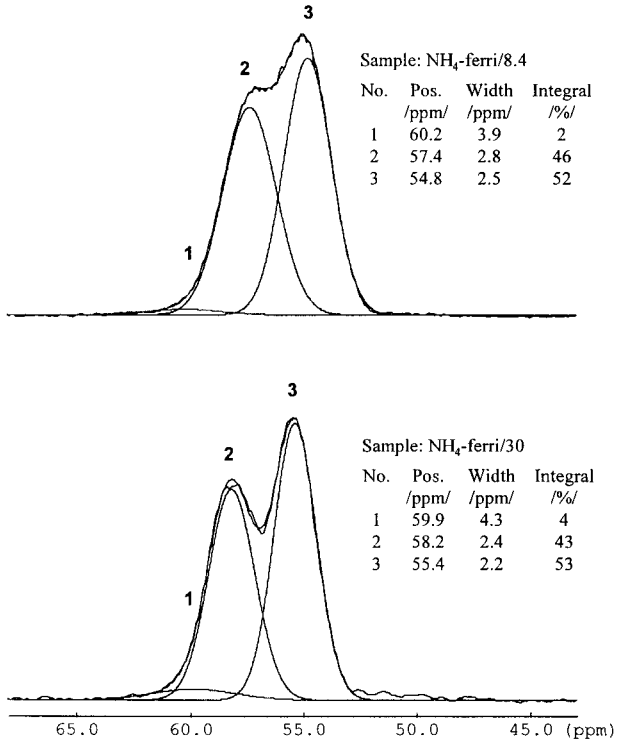

Figure 5. Isotropic (F1) projections of the ^{27}Al 5Q (MQ)MAS NMR spectra of samples NH_4-ferri/30 and NH_4-ferri/8.4 together with simulations and simulation parameters. Line positions are not corrected to the quadrupolar shift.

the sites Si(3) + Si(2) and the sites of the type T(B) comprising the sites Si(5) + Si(1) + Si(4) (notation as in ref 13) of the calcined form of siliceous ferrierite, with intensity ratios of 44.4% (2 + 2 = 4) and 55.6% (2 + 1 + 2 = 5), and average chemical shifts −112.1 and −116.6, respectively.[13] It is clear that the ratio of the intensities and the CS of the main peaks in the ^{29}Si MAS NMR spectrum of the NH_4-ferri/30, 44.3% for −112.2 ppm peak (lines 5+6) and 55.7% for the −116.6 peak (lines 7+8), matches very well with the ratio of the peaks and CS from the siliceous ferrierite. Therefore, we can assign the −112.2 ppm peak to site T(A) and the −116.6 peak to site T(B). The main peaks of sample NH_4-ferri/30 (−112.2 and −116.6 ppm) cannot be simulated by only one Gaussian line, but two. This reflects the disorder in the framework caused by the Al substitution (see below).

^{27}Al 5QMAS NMR of NH_4-Ferri/30. The F1 projection of the 2D 5Q (MQ)MAS NMR spectrum of NH_4-ferri/30 shows two well-resolved peaks with a ratio of 47% for sites A (lines 1 + 2) to 54% for sites B (line 3), respectively. The ^{29}Si NMR spectrum gave almost the same ratio for the distribution of the two silicon sites (T(A) and T(B)). The average T−O−T bond angles, calculated from the ^{27}Al isotropic chemical shifts, are 148.7° ± 0.3° for site A and 154.3° ± 0.3° for site B, which are in reasonable agreement with the T−O−T angles calculated from the ^{29}Si data (see Table 2). On the basis of the intensity ratios and the values for the average T−O−T bond angles, we assign the Al sites of type A to the site T(A) (T(3) + T(2)) and the Al sites of type B to the T(B) site (T(5) + T(1) + T(4)). As one can see from Table 2, the T−O−T angles calculated from the chemical shifts of lines 6 and 8 in the ^{29}Si NMR spectrum of NH_4-ferri/30 are not in full agreement with those of sites A and B from the ^{27}Al NMR spectrum, but if we use the chemical shifts of the less-shielded shoulders (lines 5 and 7, respectively), then the match is better. Moreover, the latter chemical shifts are similar to those from the Si(0Al) sites of the sample NH_4-ferri/8.4, i.e., they represent the Si(0Al) sites from the regions of considerably lower Si/Al ratio than 33, and therefore "feel" the presence of Al sites in the second and third coordination spheres. This indicates that in NH_4-ferri/30 there is some zoning of aluminum, leading to unit cells with no Al atoms and to unit cells with 1−2 Al atoms (Si/Al = 24), but the average Si/Al is still 33 with the aluminum randomly distributed over the possible T sites in the unit cell (UC). We have to admit that "randomly" is not fully correct, because there still is a possibility that T(3) (or T(2)) and T(5) (or T(1) and T(4)) sites might be preferentially occupied by Al atoms, but we are not able to prove it due to low resolution caused by disorder.

^{29}Si MAS NMR Spectrum of NH_4-Ferri/8.4. The spectrum (Figure 2), where the Al content is considerably higher than in NH_4-ferri/30, gives three main peaks, where the central one is a superposition of Si(1Al) and Si(0Al) sites. Assuming the random distribution of Al (i.e. the Si(0Al) peaks have the ratio 4:5), we get the simulation given in Figure 2. The ^{27}Al NMR analysis showed (see below) that this assumption was correct. Line no. 1 at −98.8 ppm is assigned to Si(2Al) sites[26] and line no. 2 at −101.8 ppm is assigned either to the defect sites (SiOH) or to the Si(1Al) sites, lines 3 and 4 are assigned to Si(1Al) sites, and lines 5 and 6 are assigned to Si(0Al) sites. The Si/Al ratio calculated from the ^{29}Si NMR results is 8.4. If we assign the −101.8 ppm peak to Si(1Al) sites, then we get Si/Al = 7.9. These results are in reasonable agreement with the chemical analysis (see Table 1).

^{27}Al 5QMAS NMR of NH_4-Ferri/8.4. In NH_4-ferri/8.4, the resolution of the F1 projection of the ^{27}Al 2D 5Q (MQ)MAS NMR spectrum is considerably lowered (the line widths have increased) due to induced disorder, but the ratio of the peaks A

(line 1 + 2) and B (line 3) remains 48%−52%, respectively (Figure 5). They are assigned to sites T(A) and T(B) in analogy with NH_4-ferri/30. Aluminum is randomly distributed between the T(A) and T(B) sites, keeping the ratio 4:5 between them. Therefore we consider the assumption of random aluminum distribution, used in the simulations of the ^{29}Si NMR spectra, to be correct. The average T−O−T angle for the Al sites of NH_4-ferri/8.4 has increased about 1° compared to NH_4-ferri/30, but at the same time the Si T−O−T angles have decreased, which must be the result of the higher Al concentration. Another quite remarkable feature is that line widths of the lines in the ^{29}Si and ^{27}Al NMR spectra, which characterize the distribution of the average T−O−T angles of the sites, are similar in the case of NH_4-ferri/30, which is in line with the findings for the HZSM-5 zeolite.[18] But in the case of NH_4-ferri/8.4, the line widths from ^{29}Si NMR spectra are considerably broader compared to ^{27}Al spectrum. Consequently, disorder around tetrahedral silicon sites is larger than that around aluminum sites.

Takaishi et al.[14] proposed that Al is exclusively located in the 6-member rings (three Al atoms), which connect the two 10-member rings of ferrierite structure. We cannot agree with that because in that case only T(1) and T(5) sites would be occupied by Al atoms, but we have shown that also T(2) and T(3) sites are involved. But still there remains the possibilty that two Al atoms are located in the 6M rings. Some of them can be Al−O−Si−O−Al type pairs. NH_4-ferri/8.4 has Si/Al ratio 8.4, so each UC contains on the average 3.8 Al atoms. We also know that about 1.6%−2.2% of the Si atoms are in Si(2Al) sites (Figures 2 and 5). Each Al−O−Si−O−Al type pair generates one Si(2Al) and six Si(1Al) sites. Each single Al site generates four Si(1Al) sites. Having the ratio of Si(2Al) and Si(1Al) sites from the ^{29}Si MAS NMR spectrum, we obtain that about 25%−35% of Al is taking part in such pairs, so one UC can contain a maximum of one Al pair or there is one Al pair for the two UC's. To obey these constraints and the rule that five-member ring cannot contain two Al atoms,[14] the pairs have to be located in the six-member rings, which form the small six-member ring "channels" along the [100], or one Al atom from the pair is located in the six-member ring. We are aware that the above reasoning is dependent on the assignment of the −98.8 ppm peak to the Si(2Al) sites and that relative intensity of this peak is very low. But, −98.8 ppm peak has been assigned to Si(2Al) sites also before,[24] and the ^{29}Si MAS NMR spectrum of the NH_4-ferri/30 does not have this peak.

Na^+-Exchanged Ferrierites. The ^{29}Si MAS NMR spectra of Na^+-exchanged samples, NH_4Na-ferri/8.4-14 and NH_4Na-ferri/8.4-83 (Figure 6), exhibit also three maxima similar to NH_4-ferri/8.4, but in the case of NH_4Na-ferri/8.4−83 they are not so well-resolved, which is the result of 83% NH_4^+ exchanged to Na^+. It is interesting to note that 14% of Na^+ exchange (NH_4-Na-ferri/8.4-14) has practically no effect on the ^{29}Si MAS NMR spectrum. The Si/Al ratio values calculated from the simulations are in reasonable agreement with the ones calculated from the chemical analysis data (Table 1). We see that in the case of ferrierite-type zeolites we are able to register the changes induced in the framework by the cation exchange, but ^{29}Si MAS NMR remains too insensitive to give any meaningful information about the physical or chemical changes near the Al sites.

From the ^{27}Al MAS NMR spectra we see that upon cation exchange the shoulder at 56 ppm gradually vanishes and the maximum shifts to 55 ppm in the case of the NH_4Na-ferri/8.4-83 (Figure 3). The ^{27}Al 2D 5Q (MQ)MAS NMR method

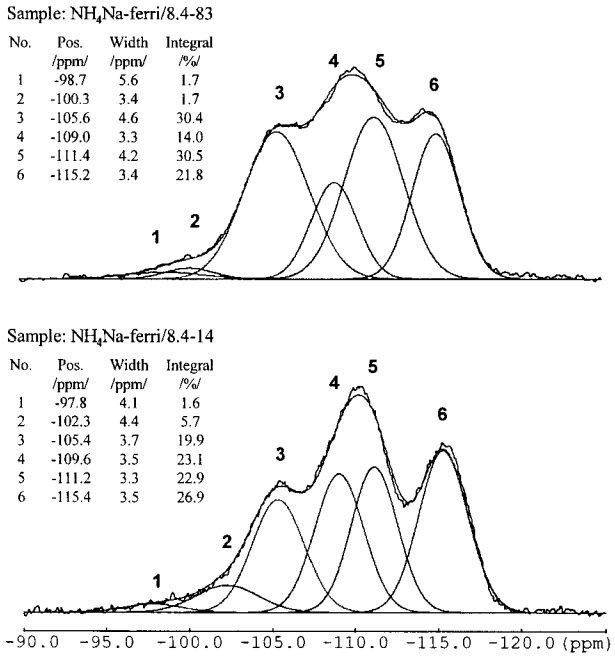

Figure 6. ^{29}Si MAS NMR spectra of samples NH_4Na-ferri/8.4-14 and NH_4Na-ferri/8.4-83 together with simulations.

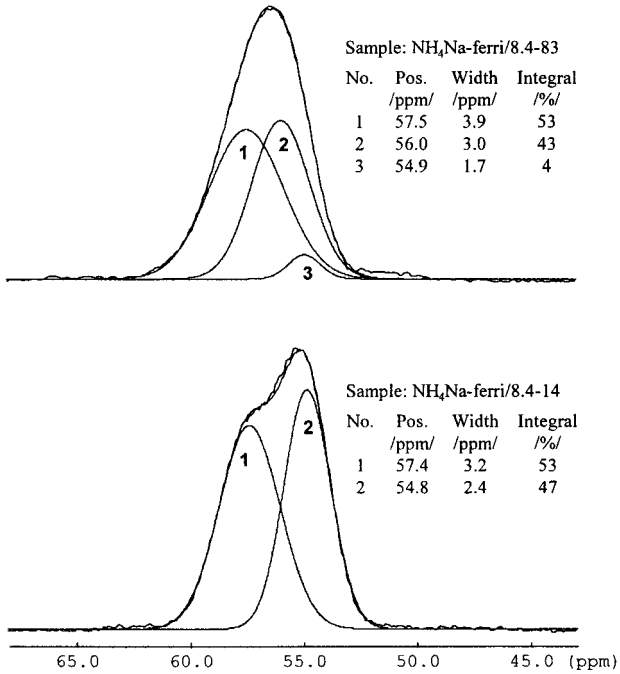

Figure 7. Isotropic (F1) projections of the ^{27}Al 5Q (MQ)MAS NMR spectra of samples NH_4Na-ferri/8.4-14 and NH_4Na-ferri/8.4-83 together with simulations and simulation parameters. Line positions are uncorrected to the quadrupolar shift.

enables a more precise characterization of this phenomenon (Figures 4 and 7, Table 2). The isotropic projection of the NH_4-Na-ferri/8.4−14 can be still simulated by two peaks, but the ratio of the two sites has changed (Figure 7). The spectrum has lost intensity on the high-field side and gained intensity on the low-field side (Figure 8). In the case of sample NH_4Na-ferri/8.4-83, the effect is even more pronounced—peak 3 (site T(B)) has almost completely vanished from the spectrum. We see that upon Na^+ exchange the T−O−T angles of the T(B) sites (T(1), T(4), and T(5)) have decreased, these are mostly the sites located in the six-member rings. Moreover, siliceous ferrierite showed similar increase of the ^{29}Si chemical shift of

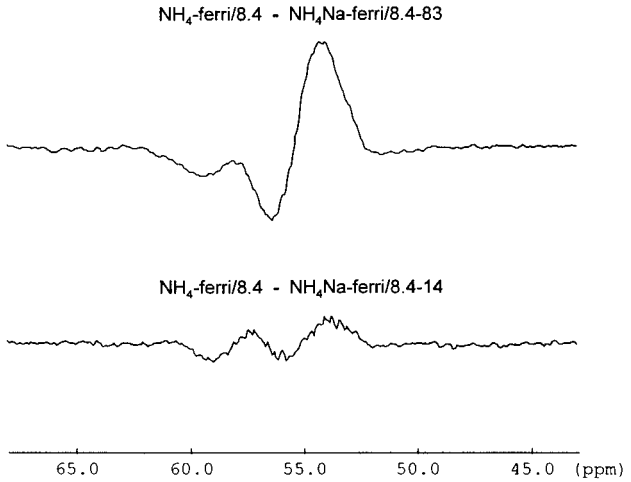

Figure 8. Difference of the isotropic (F1) projections: sample NH_4-Na-ferri/8.4-14 subtracted from NH_4-ferri/8.4 and NH_4Na-ferri/8.4-83 from NH_4Na-ferri/8.4. Prior the subtraction, the spectrum of NH_4Na-ferri/8.4-83 was shifted 0.1 ppm to higher field because of the higher F1 quadrupolar shift.

about 2 ppm (3.5°) for the Si(1) and Si(5) sites, when the ferrierite channels were filled with template molecules.[13] It is known that Na^+ exchange makes the ferrierite framework more resistant to the dealumination during steaming.[25] We have shown that Na^+ exchange has the biggest effect on the T(B) (or T(1), T(4), and T(5)) sites, most of them belonging to the six-member rings. We believe that the aluminum sites in the six-member rings play the crucial role in determining the physical and chemical properties of the aluminosilicate ferrierites. Probably the most fragile parts of the framework are the six-member rings containing two aluminum atoms.

^{23}Na MAS NMR. To find out the possible location of the Na^+ cations, we prepared two Na/NH_4-ferrierite samples: NH_4-Na-ferri/8.4-20 with 20% of Na^+ and NH_4Na-ferri/8.4-100 with 100% of Na^+. Their ^{23}Na 2D 3Q 2D (MQ)MAS NMR spectra are given in the Supporting Information. Both spectra exhibit a distribution of Na^+ cations, while NH_4Na-ferri/8.4-20 gives also intense spinning sidebands. In the spectrum of NH_4Na-ferri/8.4−100, these sidebands are almost missing, probably due to rapid exchange between the sites. We derived approximate quadrupolar coupling parameters and chemical shifts from the 2D spectra and used these data to simulate the 1D ^{23}Na MAS NMR spectra, which were recorded at higher magnetic field to supress the quadrupolar effects as much as possible (Figure 9). As one can see from the spectra and simulations, there are two types of cation sites in the samples. Both sites exhibit distribution and one of them (site SII: line 2 in Figure 9) has higher quadrupolar coupling than the other. Upon increase of the Na^+ content, the relative amount of site SII decreases, therefore we conclude that site SII is occupied preferentially at lower loadings of Na^+. Higher quadrupolar coupling and more negative chemical shift of site SII is an indication of more restricted environment than in the case of site SI (line 1 in Figure 9). Therefore, we assign site SII to be inside the "ferrierite cage", formed at the intersection of six-member and eight-member ring channels. Site SI is inside the channels formed by the 10-member rings. Sites inside the "ferrierite cage" are exchanged preferentially, and at 100% of Na^+ exchange about 35% of the cation sites remain outside the "ferrierite cage" in the 10-member ring channels. In the case of a random distribution, the ratio should be 50% inside the "ferrierite cages" and 50% in the 10-member ring channels. The explanation to the uneven distribution of Na^+ ions can be our finding that

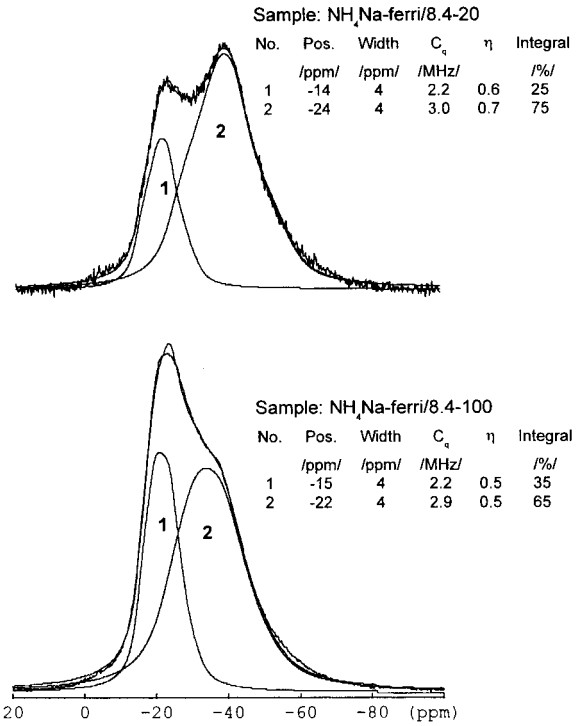

Figure 9. ^{23}Na MAS NMR spectra of samples NH_4Na-ferri/8.4-20 and NH_4Na-ferri/8.4-100 together with simulation parameters. Magnetic field 500 MHz ^{1}H NMR frequency.

approximately 30% of Al atoms are forming Al−O−Si−O−Al type pairs, located in the six-member rings. Na^+ ions, needed to neutralize the charge, coordinate the rings from both sides and therefore gather in the "ferrierite cages". Another effect of such "crowding" is the distortion of the framework, induced by electrostatic and steric repulsion, reflected by the changes in the ^{27}Al NMR spectra.

Conclusions

Combining the ^{29}Si MAS NMR and the ^{27}Al MQMAS NMR gave us the possibility to study the distribution of Al atoms between the tetrahedral framework positions. Two ferrierites, with low and high Al content in the framework, were studied. The NH_4-ferrierite (Si/Al 33) has two distinct tetrahedral aluminum sites T(A) and T(B) with an approximate ratio 4:5, which implies a random distribution between the T(A) and T(B) sites. The sites T(A) and T(B) were assigned to T(2) + T(3) and T(4) + T(1) + T(5) framework sites, respectively. We were unable to resolve the T(A) and T(B) sites any further due to line broadening generated by disorder, introduced by the Al substitution of the silicate framework. There exists some zoning of aluminum in our sample with Si/Al 33, leaving some regions of the framework without aluminum atoms and the other regions with one to two aluminum sites per UC with approximate composition of Si/Al 24.

In the ferrierite with the higher aluminum content (Si/Al 8.4) the ratio of the T(A) and T(B) sites remained 4:5. About 25%−37% of aluminum sites are located in the Al−O−Si−O−Al groups, and at least one Al from such group is located in the six-member ring, which blocks the "ferrierite cage". Higher resolution of the ^{27}Al MQMAS NMR method enabled the study of the influence of Na^+ ion exchange on the tetrahedral framework Al sites. As a result of Na^+ exchange the average T−O−T angles of T(B) aluminum sites, located mostly in the six-member rings, decrease, and framework sites with smaller T−O−T angles are generated.

By applying the ^{23}Na MQMAS NMR method to probe the Na^+ siting in the dehydrated ferrierites with different Na^+/NH_4^+ ratios, we found that Na^+ cations are preferentially located in the "ferrierite cages" and the rest of them in the 10-member ring channels.

Acknowledgment. Financial support for this work was provided by the European Commission through the Copernicus Grant CIPA CT94-0184. P.S. acknowledges support from the Estonian Science Foundation under Grant No. 2302. The authors also gratefully acknowledge Dr. Christian Fernandez at the University of Lille for the AU program that sheared the (MQ)-MAS NMR spectra.

Supporting Information Available: Sheared ^{23}Na 2D 3Q (MQ)MAS NMR spectra of samples NH_4Na-ferri/8.4-20 and NH_4Na-ferri/8.4-100 together with projections; magnetic field 360 MHz ^{1}H NMR frequency (1 page). Ordering information is given on any current masthead page.

References and Notes

(1) Haggin, J. *Chem. Eng. News* **1993**, *365*, 239.
(2) Mooiweer, H. H.; deJong, K. P.; Kraushaar-Czarnetzki, B.; Stork, W. H. J.; Krutzen, B. C. H. In *Zeolites and Related Microporous Materials: State of the Art 1994; Weitkamp, J., et al., Eds. Studies Surface Science and Catalysis*; 1994; Vol. 84C, p 2327.
(3) Li, Y.; Armor J. N. *J. Catal*. **1994**, *150*, 376.
(4) Dêdecek, J.; Sobalik, Z.; Tvarúzkova, Z.; Kaucky, D.; Wichterlová, B. *J. Phys. Chem.* **1995**, *99*, 16327.
(5) Wichterlová, B.; Dêdecek, J.; Vondrová, A. *J. Phys. Chem.* **1995**, *99*, 1065.
(6) Wichterlová, B.; Dêdecek, J.; Sobalík, Z.; Vondrová, A.; Klier, K. *J. Catal*. **1997**, *169*, 194.
(7) Wichterlová, B.; Sobalík, Z. *Catal. Today*, in press.
(8) Wise, W. S.; Tschernich, R. W. *Am. Mineral.* **1976**, *61*, 60.
(9) Vaughan, P. A. *Acta Crystallogr*. **1966**, *21*, 983.
(10) Gramlich-Meier, R.; Meier, W. M.; Smith, B. K. *Z. Kristallogr*. **1984**, *169*, 201.
(11) Alberti, A.; Sabelli, C. *Z. Kristallogr*. **1987**, *178*, 249.
(12) Morris, R. E.; Weigel S. J.; Henson, N. J.; Bull, L. M.; Janicke, M. T.; Chmelka, B. F.; Cheetham, A. K. *J. Am. Chem. Soc.* **1994**, *116*, 11854.
(13) Lewis, Jr., J. E.; Freyhardt, C. C.; Davis, M. E. *J. Phys. Chem*. **1996**, *100*, 5039.
(14) Takaishi, T.; Kato, M. *Zeolites* **1995**, *15*, 21.
(15) Engelhardt, G.; Michel, D. *High-Resolution Solid-State NMR of Silicates and Zeolites*; John Wiley & Sons: Chichester, 1987.
(16) Frydman, L.; Harwood, J. S. *J. Am. Chem. Soc*. **1995**, *117*, 5367.
(17) Fernandez, C.; Amoureux, J. P. *Chem. Phys. Lett.* **1995**, *242*, 449.
(18) Sarv, P.; Fernandez, C.; Amoureux, J. P.; Keskinen, K. *J. Phys. Chem*. **1996**, *100*, 19223.
(19) Hunger, M.; Sarv, P.; Samoson, A. *Solid State Nucl. Magn. Reson.*, in press.
(20) Massiot, D.; Touzo, B.; Trumeau, D.; Coutures, J. P.; Virlet, J.; Florian, P. Grandinetti P. J. *Solid State Nucl. Magn. Reson.* **1996**, *6*, 73.
(21) Amoureux, J. P.; Fernandez, C. Proceedings of the 38th ENC, Orlando, FL, 1997; ENC: Santa Fe, 1997; p 150.
(22) Lippmaa, E.; Samoson, A.; Mägi, M. *J. Am. Chem. Soc*. **1986**, *108*, 1730.
(23) Thomas, J. M.; Kennedy, J.; Ramdas, S.; Hunter, B. K.; Tennakoon, D. T. B. *Chem. Phys. Lett*. **1983**, *102*, 158.
(24) Gabelica, Z.; Nagy, J. B.; Bodart, P.; Debras, G.; Derouane, E. G.; Jacobs, P. A. In *Zeolites: Science and Technology*; Ribeiro, R. F. et al., Eds.; Martinus Nijhoff Publishers: The Hague, 1984; p 193.
(25) Xu, W. Q.; Yin, Y. G.; Suib, S. L.; Edwards, J. C.; O'Young, C. L. *J. Catal.* **1996**, *163*, 232.